DOI: 10.1017/S1341927605503702
Microsc Microanal 11(Suppl 2), 2005

Three-dimensional arrangement of rare-earth atoms at grain boundaries in silicon nitride ceramics using aberration-corrected HAADF-STEM

G. B. Winkelman*, C. Dwyer*, T. S. Hudson*, D. Nguyen-Manh*, M. D blinger*, R. L. Satet**, M. J. Hoffmann,** and D. J.H. Cockayne*

*Department of Materials, University of Oxford, Parks Road, Oxford OX1 3PH, UK.
**Institut f r Keramik im Maschinenbau, Universit t Karlsruhe, D-76131 Karlsruhe, Germany.

Used as sintering aids in the production of Si_3N_4 ceramic components, rare-earth elements promote the growth of thin, needle-like grains [1], upon which the elevated toughness and strength [2] of these advanced materials rely. However, rare-earth additions differ in their effectiveness *e.g.* for crystals grown in a glass matrix [3], La additions result in an average grain aspect ratio five times that exhibited by specimens containing Lu. To explore the impact of rare-earth additions, we determine the three-dimensional arrangement of rare-earth atoms (La, Sm, Yb and Lu) extending into the amorphous phase (both intergranular films and pockets) at prismatic interfaces in polycrystalline Si_3N_4. This is achieved using aberration-corrected high-angle annular dark-field scanning transmission electron microscopy [4] (HAADF-STEM) and image processing.

HAADF-STEM images were obtained using a unique JEOL 2200FS TEM/STEM fitted with aberration-corrected probe-forming and objective lenses, such that the images were formed in a virtually Cs-free environment. A probe convergence semi-angle of 16 mrad was used; the diameter of the probe was < 0.17 nm; the inner and outer semi-angles of the HAADF detector were ≈ 50 and 140 mrad, respectively. In a STEM, the intensity of electrons scattered to high angles is relatively low compared to the low-angle scattered electron intensity, and hence experimental HAADF-STEM images are intrinsically noisy. Furthermore, raw images are often distorted due to specimen drift during image acquisition and instabilities in the probe scanning system. Hence, post-acquisition image processing (Fig. 1) is helpful. Periodically averaged HAADF-STEM images of grain-intergranular film interfaces (upper row of images in Fig. 2) are presented for all compositions, viewed parallel to mutually perpendicular [001] and [100] directions. Displayed immediately below the upper row of images in Fig. 2 are analogous grain-pocket interfaces. The Si_3N_4 crystal terminates as a row of half-hexagons when projected parallel to [001], and any evidence of structure beyond the row of half-hexagons is likely to represent rare-earth atoms in preferred positions in the amorphous phase. Up to five inequivalent preferred positions were observed (*e.g.* Sm, see Fig. 2) parallel to [001]. These positions are the same (within experimental error) independent of whether the crystal-amorphous interface was that of a grain-intergranular film or a grain-pocket. Observation parallel to [100] provides the third atomic coordinate of the preferred atomic positions unavailable from [001]. While the atomic arrangement in the amorphous phase conforms to the periodicity of the terminating crystal plane in all four cases, the attachment sites are very different for the different additives. In this work, atomic positions in the amorphous phase are presented as distances from a defined origin in the crystalline phase, and are determined to within ≈ 0.02 nm in three dimensions. We demonstrate that aberration-corrected HAADF-STEM combined with post-acquisition image processing leads to an unprecedented level of accuracy in the description of extended atomic structure in an amorphous phase adjacent to a crystal. The combination of these techniques is eminently suited to the characterisation of other functional materials and nanostructures, *e.g.* doped amorphous gate-oxide layers on silicon substrates.

References

[1] Kramer, M., Hoffmann, M.J., and Petzow, G. Grain growth studies of silicon nitride dispersed in an oxynitride glass. *J. Am. Ceram. Soc.* **76,** 2778-2784 (1993).
[2] Becher, P.F., *et al.* Microstructural design of silicon nitride with improved fracture toughness: I, Effects of grain shape and size. *J. Am. Ceram. Soc.* **81,** 2821-2830 (1998).
[3] Satet, R.L. and Hoffmann, M.J. Grain growth anisotropy of beta-silicon nitride in rare-earth doped oxynitride glasses. *J. Eur. Ceram. Soc.* **24,** 3437-3445 (2004).
[4] Pennycook, S.J. and Jesson, D.E. High-resolution Z-contrast imaging of crystals. *Ultramicroscopy* **37,** 14-38 (1991).
[5] Financial support from the European Community Growth Program (Contract No. G5RD-CT-2001-00586) and the NSF (Grant No.\ DMR-0010062) is gratefully acknowledged.

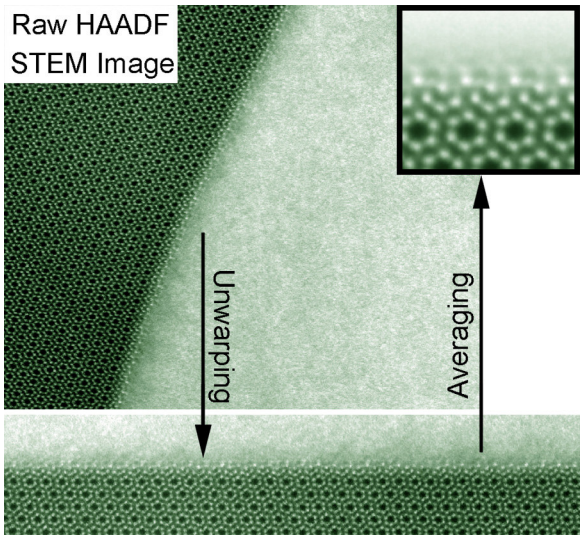

Fig. 1. Image distortion correction and subsequent periodic averaging. The distortion of the 2-dimensional lattice of the oriented crystal was determined by cross-correlation with a thin strip (~0.2 x 2.0 nm) with long axis parallel to the scanning direction. The distorted 2-dimensional lattice was mapped onto a regular lattice, and bilinear interpolation of this lattice map was used for points between the lattice points. For the averaging, N repeat units were used (N ≈ 30), resulting in a $\sqrt{N}$ enhancement of the signal to noise ratio. Each averaged image consists of several identical repeat units

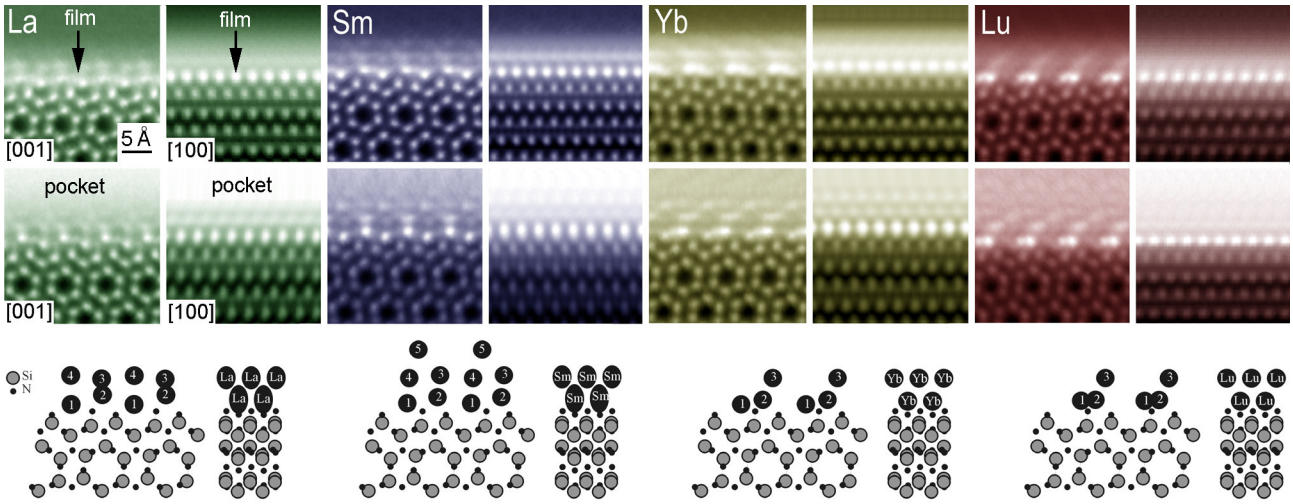

Fig. 2. Averaged images of both grain-intergranular film interfaces (upper row of images) and grain-pocket interfaces (immediately below upper row of images). For each rare-earth additive (La, Sm, Yb, Lu), images represent the projected structure parallel to both [001] and [100]. Schematic representation of the atomic positions of all species is provided.

https://doi.org/10.1017/S1431927605503702 Published online by Cambridge University Press